Taylor & Francis
Taylor & Francis Group

CLINICAL STUDY

OPEN ACCESS | Check for updates

PFKFB3 downregulation aggravates Angiotensin II-induced podocyte detachment

Xiaoxiao Huang[a#], Zhaowei Chen[a,b#], Zilv Luo[a], Yiqun Hao[a], Jun Feng[a], Zijing Zhu[a], Xueyan Yang[a], Zongwei Zhang[a,b], Jijia Hu[a,b], Wei Liang[a,b] and Guohua Ding[a,b]

[a]Division of Nephrology, Renmin Hospital of Wuhan University, Wuhan, China; [b]Nephrology and Urology Research Institute of Wuhan University, Wuhan, China

ABSTRACT

Podocytes play a critical role in maintaining normal glomerular filtration, and podocyte loss from the glomerular basement membrane (GBM) initiates and worsens chronic kidney disease (CKD). However, the exact mechanism underlying podocyte loss remains unclear. Fructose-2,6-biphosphatase 3 (PFKFB3) is a bifunctional enzyme that plays crucial roles in glycolysis, cell proliferation, cell survival, and cell adhesion. This study aimed to determine the role of PFKFB3 in angiotensin II (Ang II) kidney damage. We found that mice infused with Ang II developed glomerular podocyte detachment and impaired renal function accompanied by decreased PFKFB3 expression *in vivo* and *in vitro*. Inhibition of PFKFB3 with the PFKFB3 inhibitor 3PO further aggravated podocyte loss induced by Ang II. In contrast, activating PFKFB3 with the PFKFB3 agonist meclizine alleviated the podocyte loss induced by Ang II. Mechanistically, PFKFB3 knockdown likely aggravate Ang II-induced podocyte loss by suppressing talin1 phosphorylation and integrin beta1 subunit (ITGB1) activity. Conversely, PFKFB3 overexpression protected against Ang II-induced podocyte loss. These findings suggest that Ang II leads to a decrease in podocyte adhesion by suppressing PFKFB3 expression, and indicates a potential therapeutic target for podocyte injury in CKD.

1. Introduction

Terminally differentiated glomerular visceral epithelial cells (also known as podocytes) are located in the outer glomerular basement membrane (GBM) [1] that plays a key role in maintaining normal glomerular filtration [2,3]. Podocyte detachment from the glomerular basement membrane is an important feature of chronic kidney disease (CKD) [4] and it leads to proteinuria and CKD progression [5,6]. Apoptosis is considered a common mechanism of podocyte loss, but most data have been generated *in vitro*, and evidence of podocyte apoptosis *in vitro* is scant [7]. Podocyte detachment is not the result of apoptosis but precedes it [8].

Angiotensin II (Ang II) promotes podocyte detachment [9], but the exact mechanism remains obscure. Angiotensin II is the main effector of the renin-angiotensin system (RAS) [10,11]. The RAS is activated in various renal diseases [12,13] and is a major risk factor for CKD progression [14]. Angiotensin II was originally thought to affect renal function mainly by causing glomerular endothelial cells to alter glomerular

filtration pressure. However, Ang II actually affects renal function not only by altering hemodynamics but also by directly acting on podocytes [15].

The homodimeric and bifunctional enzyme family of phosphofructokinase-2/Fructose-2,6-bisphosphatase (PFK-2/PFKFB) promotes glycolysis by increasing levels of fructose-2,6-bisphosphate (F2,6P2), which in turn activates the key rate-limiting enzyme 6-phosphofructo-1-kinase (PFK-1) and enhances the conversion of fructose-6-phosphate (F6P) to fructose-1,6-bisphosphate (F1,6P2) in the glycolytic pathway. This causes increased glycolytic flux and increased ATP and NADH production [16]. Among the PFKFB family of four enzymes (PFKFB1-4), PFKFB3 has the highest ratio of kinase to phosphatase activity, which ensures a high glycolytic rate [17]. Recent findings have indicated that PFKFB3 exerts protective effects on the kidneys [18] and promotes the activation of cyclin-dependent kinase-1(cdk1) [19], which promotes talin1 phosphorylation [20]. Excessive talin1 phosphorylation promotes integrin beta1 subunit (ITGB1) activity

on the cell surface [21]. Active ITGB1 is an important adhesion molecule on the surface of podocytes, and its activation enhances podocyte adhesion capacity [22–25]. Inhibiting PFKFB3 significantly reduces the expression of cell adhesion molecules, resulting in diminished cell adhesion [26–29]. Therefore, we speculated that Ang II could inhibit talin1 phosphorylation and ITGB1 activation through downregulating PFKFB3 expression. Therefore, we investigated the role of PFKFB3 in Ang II-induced podocyte injury and identified a novel target for CKD treatment.

2. Materials and methods

2.1. Establishment of Ang II-infused mouse model

C57BL/6 mice were acclimatized in a controlled environment under standard temperature and humidity and provided access to food and water *ad libitum* for one week. Twenty-four 8-week-old C57BL/6 mice (weight, 18–22 g) were randomly allocated to the following experimental groups (*n* = 6 per group): normal saline (NS) infused using a subcutaneous micro-osmotic pump; 700 ng/kg/min of Ang II (HY-13948; MedChem Express, Monmouth Junction, NJ, USA) infused by the pump for 4 weeks; Ang II (700 ng/kg/min) infused by the pumps plus a daily intraperitoneal injection of 70 mg/kg of the PFKFB3 inhibitor 3PO (A15932; Adooq Bioscience LLC., Irvine, CA, USA) [30] for 4 weeks; and Ang II (700 ng/kg/min) infused by the pump plus a daily intraperitoneal injection of 100 mg/kg of the PFKFB3 agonist meclizine (HY-B0349; MedChem Express) [31] for 4 weeks, Thereafter, urine samples and kidneys were collected from the mice. All animal experiments were approved by the Animal Ethics Committee at Renmin Hospital, Wuhan University (Wuhan, China).

2.2. Cell culture and treatments

Conditionally immortalized human podocytes provided by Dr. Moin A. Saleem, (Southmead Hospital, Bristol, UK) were cultured at 33 °C in Roswell Park Memorial Institute (RPMI) 1640 medium (HyClone Laboratories Inc., South Logan, UT, USA) containing 10% heat-inactivated Gibco fetal bovine serum (FBS), 100 U/mL penicillin G, 100 μg/mL Invitrogen streptomycin, and 1× insulin-transferrin-selenium (ITS; all from Thermo Fisher Scientific Inc., Waltham, MA, USA). Differentiated podocytes were applied in all experiments. Podocytes were induced to differentiate in ITS-free medium at 37 °C for 10–14 days, then were stimulated with Ang II (10 μM), 3PO (10 μM) or meclizine (50 μM) for 24 h. We then transfected the podocytes with small interfering RNA (siRNA) to target PFKFB3 (Purchased from Sangon Biotech Co., Ltd., Shanghai, China, Supplementary Table 1) using HiPerFect (301704; Qiagen GmbH, Hilden, Germany) as described by the manufacturer. The recombinant expression plasmid pEnCMV-PFKFB3 was transfected into podocytes using Lipo3000 (ThermoFisher Scientific Inc.) as described by the manufacturer. The recombinant expression plasmid, pEnCMV-PFKFB3, was constructed using the Miaoling Plasmid

Platform. All experimental results were confirmed using three independent podocyte clones.

2.3. Measurements of urinary albumin

We measured total volumes of urine collected over a period of 24 h from mice housed in metabolic cages. We eliminated debris in the urine samples by centrifugation at 2000 rpm for 3–5 min, then measured protein concentrations in the supernatant using a urine protein quantitation kit (C035-2-1; Nanjing Jiancheng Bioengineering Institute, Nanjing, China). Total 24-h urinary protein was calculated based on the volume of the collected urine and the urinary protein concentration.

Mouse urine was collected for 24 h, and centrifuged at 2000 rpm for 3–5 min. The supernatant was boiled in an SDS loading buffer for 5 min in a water bath. Protein samples were separated by 10% sodium dodecyl sulfate-polyacrylamide gel electrophoresis (SDS-PAGE) (Bio-Rad Laboratories Ins., Hercules, CA, USA) using a stained protein (26,616; Thermo Fisher Scientific Inc., USA) as the molecular weight markers. The gels were stained with Koma Brilliant Blue. Thereafter, proteins were relatively quantified by comparing grayscale values of the gels obtained from the groups and multiplying them by the volume of mouse urine collected.

2.4. Kidney histological and morphometric analyses

Mouse kidney tissues were fixed in formalin, embedded in paraffin, sectioned, and stained with hematoxylin-eosin (HE) and periodic acid-Schiff (PAS) reagent. Glomerular structures were visualized using a light microscope at 400× magnification. All slide contained five non-overlapping fields per kidney section.

2.5. Immunofluorescent staining

We used 1:200-diluted anti-PFKFB3 (ab181861; Abcam Plc., Cambridge, UK) and 1:100-diluted synaptopodin (sc-515842; Santa Cruz, Dallas, TX, USA) to detect their respective antigens in paraffin-embedded mouse kidney tissue sections. Antigens were retrieved from deparaffinized sections by immersion in citrate buffer (Epitope Retrieval Solution) Ph 6.0 for 10 min. Nonspecific antigen binding was blocked by immersion in 10% BSA for 2 h, then the sections were incubated with primary antibodies overnight at 4 °C. After incubation with secondary antibodies (A-11012, A-11034; Thermo Fisher Scientific Inc., USA) for 1 h at 37 °C, the sections were counterstained with 4',6-diamidino-2-phenylindole (DAPI). The sections were visualized using a confocal fluorescence microscope (FV1200, Olympus Corp., Tokyo, Japan), and images were acquired using a 100× objective lens. The settings for the laser power, gain, and offset were optimized for each channel and were consistent for all samples. The acquisition settings were as follows: excitation at 360 nm for DAPI, emission at 450–460 nm; excitation at 488 nm for PFKFB3,

emission at 505–550 nm; excitation at 594 nm for synaptopodin, emission at 610–650nm. Images were processed using FV10-ASW Viewer software (Olympus Corporation, Tokyo, Japan).

2.6. Western blots

Proteins were extracted by lysing the kidney cortex or incubating podocytes with RIPA buffer (Beyotime, Shanghai, China) containing 1 mM phenylmethylsulfonyl fluoride (PMSF). Stained proteins (26,616; Thermo Fisher Scientific Inc., USA, and WJ102; EpiZyme Biotechnology Inc., China) were the molecular weight markers. Total proteins (40 μg) were separated by 10% SDS-PAGE (Bio-Rad Laboratories Inc., Hercules, CA, USA), then transferred to polyvinylidene difluoride (PVDF) membranes (Millipore Merck, Burlington, MA, USA) under a constant current of 100 amps per gel for 1.5 h in an ice bath. Nonspecific binding was blocked with 5% skimmed milk for 1 h at 37 °C then the membranes were incubated with primary antibodies overnight at 4 °C. On the following day, the membranes were incubated with secondary antibodies at 37 °C for 1 h. The blots were visualized using chemiluminescent reagents (G2014-50ML; Servicebio, Wuhan, China). The following primary antibodies were all diluted 1:5000 to detect their respective antigens: anti-PFKFB3 (ab181861; Abcam Plc., UK), anti-integrin beta1 (12G10) (ab30394; Abcam Plc., UK), anti-talin1 (YP1523; Immunoway Biotechnology Co., Plano, TX, USA), anti-GAPDH (600004-1; Proteintech Group Inc., Rosemont, IL, USA), The secondary antibodies were HRP-linked goat anti-rabbit IgG and HRP-linked goat anti-mouse IgG. Target proteins were normalized to the internal standard GAPDH, then quantified by densitometry using ImageJ software (National Institutes of Health, [NIH] Bethesda, MD, USA).

2.7. Adhesion assay

Podocytes were suspended in 2 mL of serum-free culture medium and counted using a hemacytometer. Podocytes (1×10^6) were cultured in six-well plates coated with type IV collagen (C7521; Sigma-Aldrich Corp., St. Louis, MO, USA) and incubated at 37 °C for 2 h. Five wells were used for each experimental group. The plates were washed twice with phosphate-buffered saline (PBS), then adherent podocytes were fixed in 4% paraformaldehyde (PFA), stained with crystal violet, and assessed by microscopy. The numbers of adherent podocytes in each field of view were counted using ImageJ software then the count was averaged by the number of podocytes in five fields of view.

2.8. RT-PCR and RT qPCR

Total RNA was extracted from cultured podocytes using the RNA isolator Total RNA Extraction Reagent (R401-01; Vazyme Biotech Co., Ltd., Nanjing, China) as described by the manufacturer. First-strand cDNA was generated by reverse transcribing total RNA (1 μg) using NovoScript Plus All-in-one 1st Strand cDNA Synthesis SuperMix (gDNA Purge; E047-01A

Novoprotein, Shanghai, China) as described by the manufacturer. Synthesized cDNA was amplified by RT-PCR using NovoStart SYBR qPCR SuperMix Plus (E096-01A; Novoprotein, China). The expression of gapdh and pfkfb3 was assessed using the primer (sequences listed in Supplementary Table 2). Real-time PCR proceeded using a cytoflex flow cytometer (Beckman Coulter Inc., Brea, CA, USA), and the data were analyzed using the ΔΔCT method.

2.9. Apoptosis assay

Podocyte apoptosis was assessed using BD Pharmingen™ PE Annexin V Apoptosis Detection Kit I (559763; BD Biosciences San Jose, CA, USA), as described by the manufacturer.

2.10. Statistical analysis

All date were statistically analyzed using GraphPad Prism 9 (GraphPad Software Inc., San Diego, CA, USA). Statistical data are presented as means ± standard deviation. Statistical differences between groups were analyzed using the Student t-test. Statistical differences between three or more groups were analyzed using one-way ANOVA. All experiments included at least three replicates. Statistical significance was set at $p < 0.05$.

3. Results

3.1. Angiotensin II-induced podocyte detachment and impaired kidney function

Staining with PAS and HE revealed significant glomerulosclerosis in kidney sections obtained from Ang II-infused mouse models (Figure 1(A)). We then explored whether Ang II is involved in podocyte detachment. We assessed the effects of Ang II on podocyte adhesion in vivo and in vitro using the actin-associated protein synaptopodin as a specific podocyte marker [32,33]. Immunofluorescence staining revealed fewer synaptopodin-positive podocytes (Figure 1(B)) and partially fused and absent podocyte foot processes (Figure S1) in mice infused with Ang II. These changes resulted in impaired glomerular filtration and increased urinary protein excretion (Figure 1(C)). We also found decreased adhesion in podocytes stimulated with Ang II in vitro compared with controls (Figure 1(D,E)). These results indicated that Ang II-induced podocyte detachment and impairs kidney function.

3.2. Angiotensin II stimulation induced decreased PFKFB3 expression in podocytes

We evaluated the effects of Ang II on podocyte expression of PFKFB3 in vivo and in vitro. Stimulation with Ang II decreased PFKFB3 transcription in cultured podocytes (Figure S2). Immunohistochemical analysis of kidney sections using anti-PFKFB3 antibodies revealed significantly reduced PFKFB3-positive staining in Ang II-infused mice compared with controls (Figure 2(A)). Confocal microscopy and
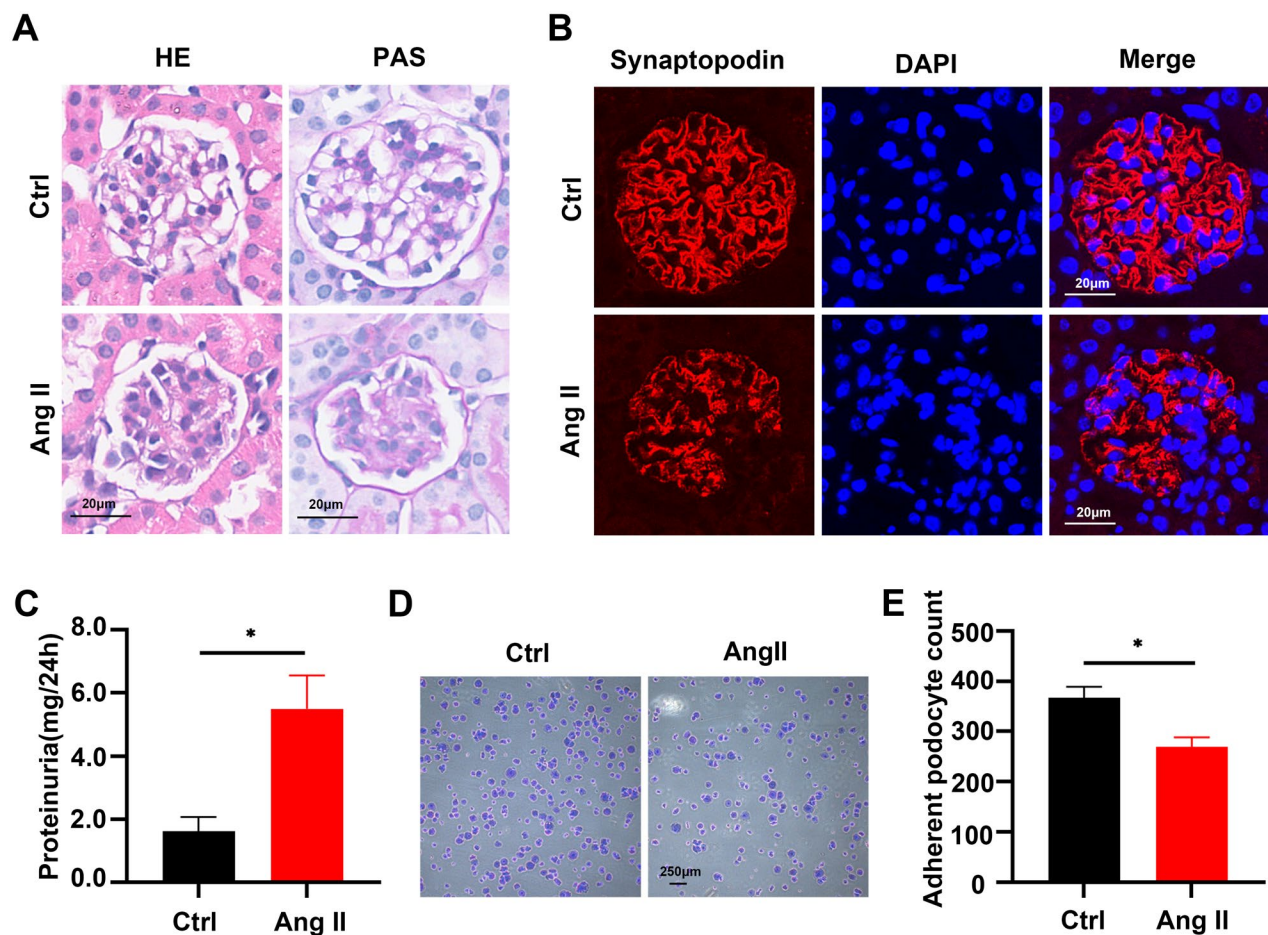
Figure 1. Angiotensin II-induced podocyte detachment and impaired kidney function. (A) Representative images of HE and PAS staining in normal saline (ctrl) and Ang II-infused mice. Scale bars:20μm. (B) Representative immunofluorescent staining of synaptopodin (podocyte-specific marker, red) and DAPI (blue) in different groups, Scale bars:20μm. (C) Quantitative determination of 24h urine Total protein (UTP) in ctrl and Ang II-infused group ($n = 6$), $*p < 0.05$. (D) Representative images of adhesion assays in ctrl and Ang II-treated podocytes in cultures. Scale bars = 250μm. (E) Quantitative determination of podocyte numbers in ctrl and Ang II-treated podocytes in cultures ($n = 5$), $*p < 0.05$.

immunofluorescence staining confirmed that Ang II inhibited PFKFB3 expression in the cytoplasm and nuclei of human podocytes *in vitro* (Figure 2(B)). Double immunofluorescence staining for PFKFB3 and synaptopodin confirmed that Ang II inhibited PFKFB3 expression in mouse glomerular podocytes (Figure 2(C)). Western blots also confirmed that Ang II inhibited PFKFB3 expression in glomeruli (Figure 2(D,F)) and cultured podocytes (Figure 2(E,G)). These results indicated that Ang II suppressed PFKFB3 expression in podocytes.

3.3. PFKFB3 participated in the regulation of adhesion molecule expression in vivo

Although Ang II affected PFKFB3 expression in podocytes, whether it functions in podocyte detachment remains unclear. We, therefore, investigated the role of PFKFB3 in podocyte adhesion *in vivo* by administering mice infused with Ang II with either 3PO or meclizine. The result showed that 3PO exacerbated, whereas meclizine reversed the Ang II-induced inhibition of synaptopodin expression in podocytes (Figure 3(A,B)). Deleting PFKFB3 similarly exacerbated the Ang II-induced decrease in synaptopodin expression

(Figure S3). These results suggested that PFKFB3 plays a role in podocyte damage induced by Ang II. We investigated levels of activated ITGB1 and talin1 phosphorylation to clarify the mechanism of action of PFKFB3 in podocyte detachment. Angiotensin II inhibited PFKFB3 expression, resulting in decreased talin1 phosphorylation and ITGB1 activity compared with saline-infused controls, and 3PO exacerbated this phenomenon (Figure 3(C,D)). Conversely, meclizine reversed the inhibition of talin1 phosphorylation and ITGB1 activity induced by Ang II (Figure 3(E,F)). These results showed that inhibiting PFKFB3 impaired podocyte adhesion, whereas upregulating it reversed the Ang II-induced decrease in podocyte adhesion.

3.4. Regulation of podocyte adhesion was mediated by PFKFB3 in vitro

We used adhesion assays *in vitro* to investigate the regulatory role of PFKFB3 in podocyte adhesion. Co-treatment of podocytes with 3PO and Ang II resulted in reduced podocyte adhesion due to inhibition of PFKFB3 expression (Figure 4(A,B)). In contrast, meclizine increased the population of
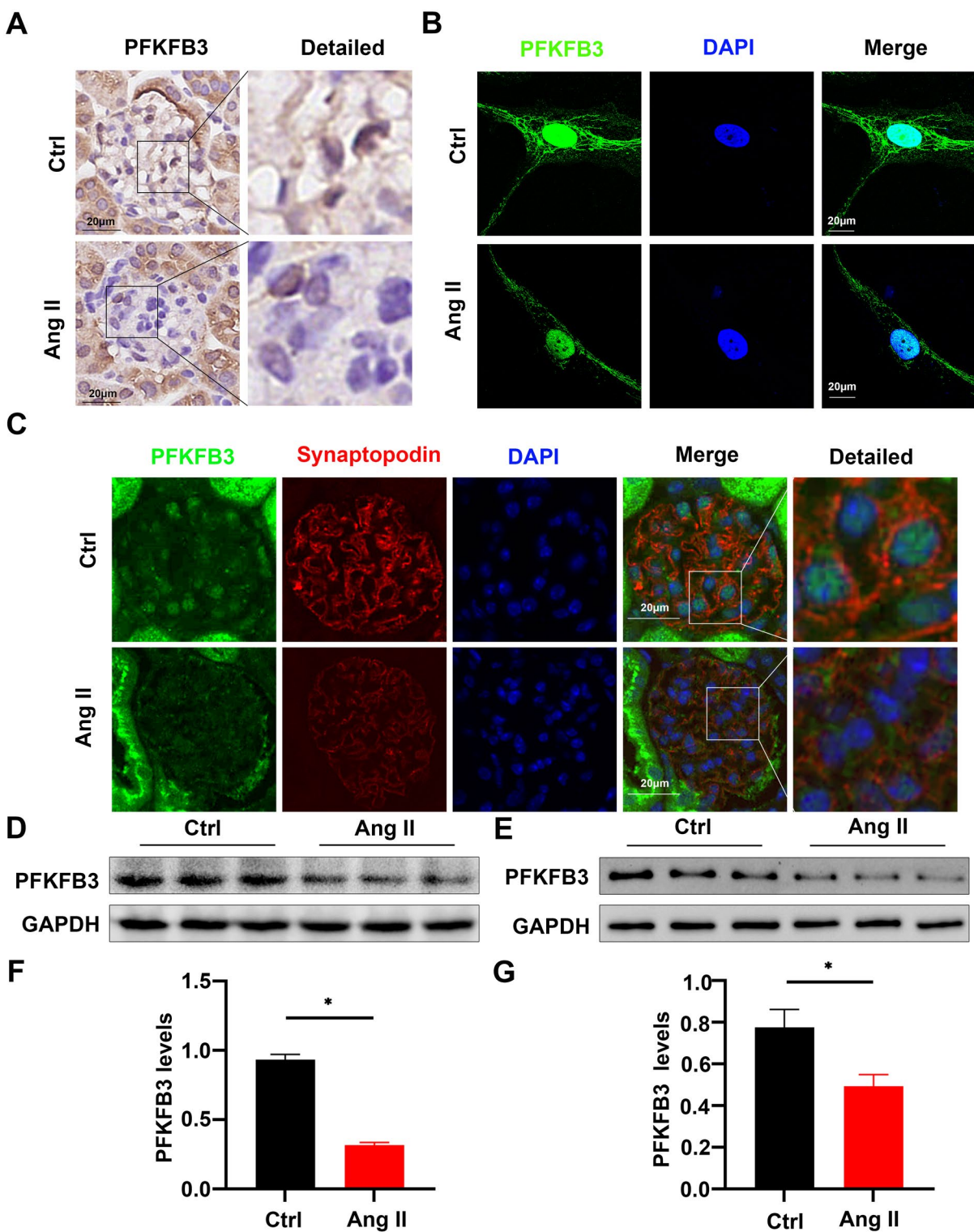
Figure 2. Angiotensin II stimulation induced decreased PFKFB3 expression in podocytes. (A) Representative Immunohistochemical staining of PFKFB3 in glomeruli from different groups. Scale bars: 20 μm. (B) Representative immunofluorescence image of PFKFB3 in ctrl and Ang II-treated podocytes in cultures obtained by confocal microscopy, Scale bars: 20 μm. (C) Representative immunofluorescent staining of PFKFB3 (green) and synaptopodin (podocyte-specific marker, red) in ctrl and Ang II-infused mice, Scale bars: 20 μm. (D) Representative Western blots of PFKFB3 in glomeruli from ctrl and Ang II-infused mice. (E) Representative Western blots of PFKFB3 in ctrl and Ang II-treated podocytes in cultures. (F) Quantitative determination of Western blots of PFKFB3 expression in ctrl and Ang II-infused mice ($n=6$), $*p<0.05$. (G) Quantitative determination of Western blots of PFKFB3 expression in ctrl and Ang II- treated podocytes in cultures ($n=3$), $*p<0.05$.
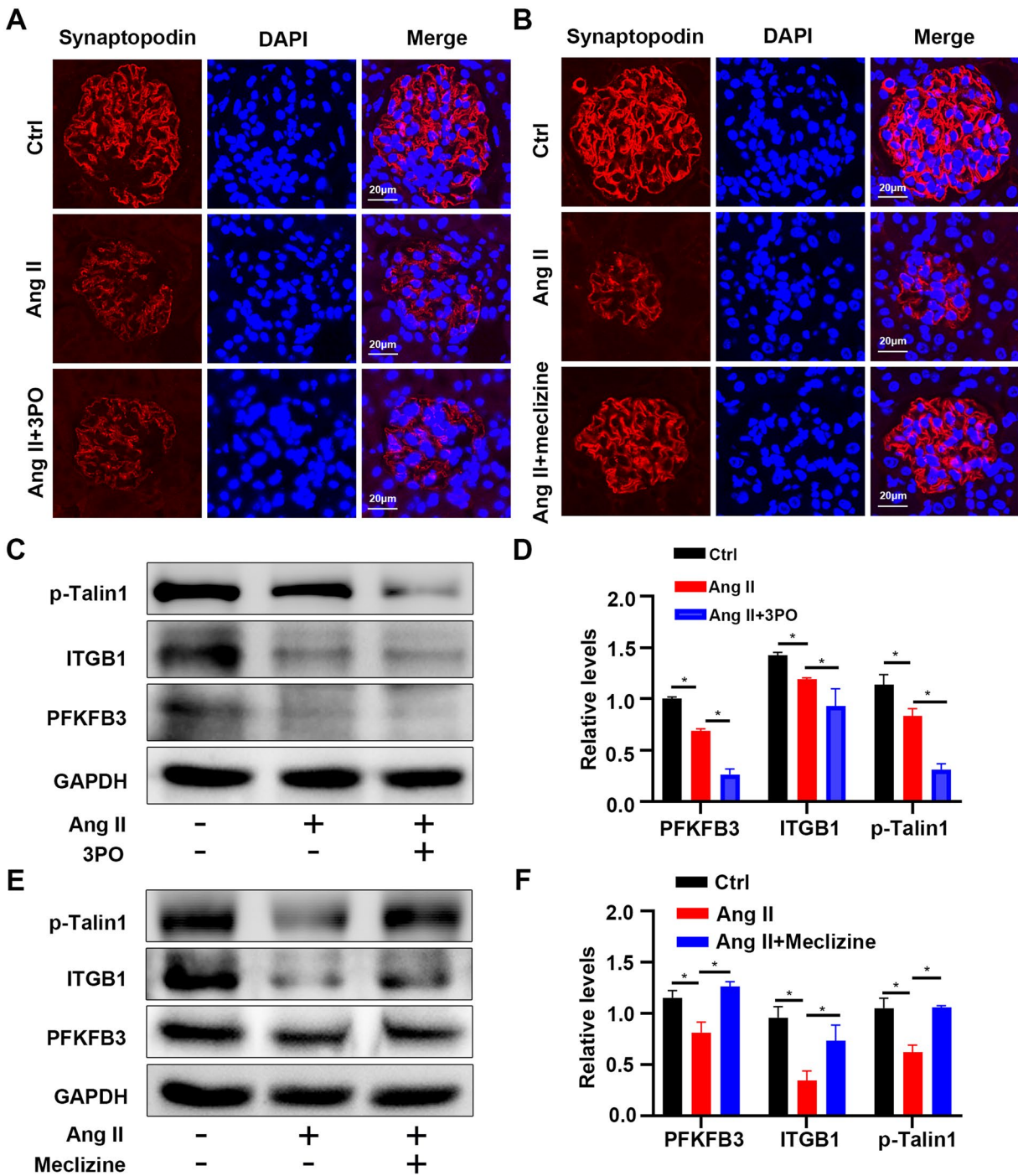
Figure 3. PFKFB3 participated in the regulation of adhesion molecule expression *in vivo*. Representative immunofluorescent staining of synaptopodin (podocyte-specific marker, red) and DAPI (blue) in 3PO (A) or meclizine (B) treated groups, Scale bars:20μm. (C) Representative Western blots of phosphorylation of Talin1 and active ITGB1, and PFKFB3 in each treatment groups of mice. (D) Quantitative determination of Western blots of PFKFB3, ITGB1, p-Talin1 expression in each group ($n=6$), *$p<0.05$. (E) Representative Western blots of phosphorylation of Talin1 and active ITGB1, and PFKFB3 in each treatment groups of mice. (F) Quantitative determination of Western blots of PFKFB3, ITGB1, p-Talin1 expression in each group ($n=6$), *$p<0.05$.

adherent podocytes stimulated by Ang II (Figure 4(C,D)). Moreover, PFKFB3 inhibition led to decreased talin1 phosphorylation and ITGB1 activity (Figure 4(E,F)). Meclizine notably reversed the Ang II-induced decrease in talin1 phosphorylation and ITGB1 activity (Figure 4(G,H)). Collectively, these results suggested that PFKFB3 may play a role in regulating podocyte adhesion *via* the p-talin1-ITGB1 pathway during Ang II-induced podocyte injury.

3.5. Angiotensin II-induced podocyte detachment in vitro is exacerbated by PFKFB3 knockdown

We investigated the effects of PFKFB3 knockdown on podocyte adhesion by transfecting podocytes with PFKFB3 siRNA *in vitro*. The population of adherent podocytes decreased after PFKFB3 knockdown (Figure 5(A,B)). Furthermore, PFKFB3 knockdown reduced PFKFB3 expression in podocytes
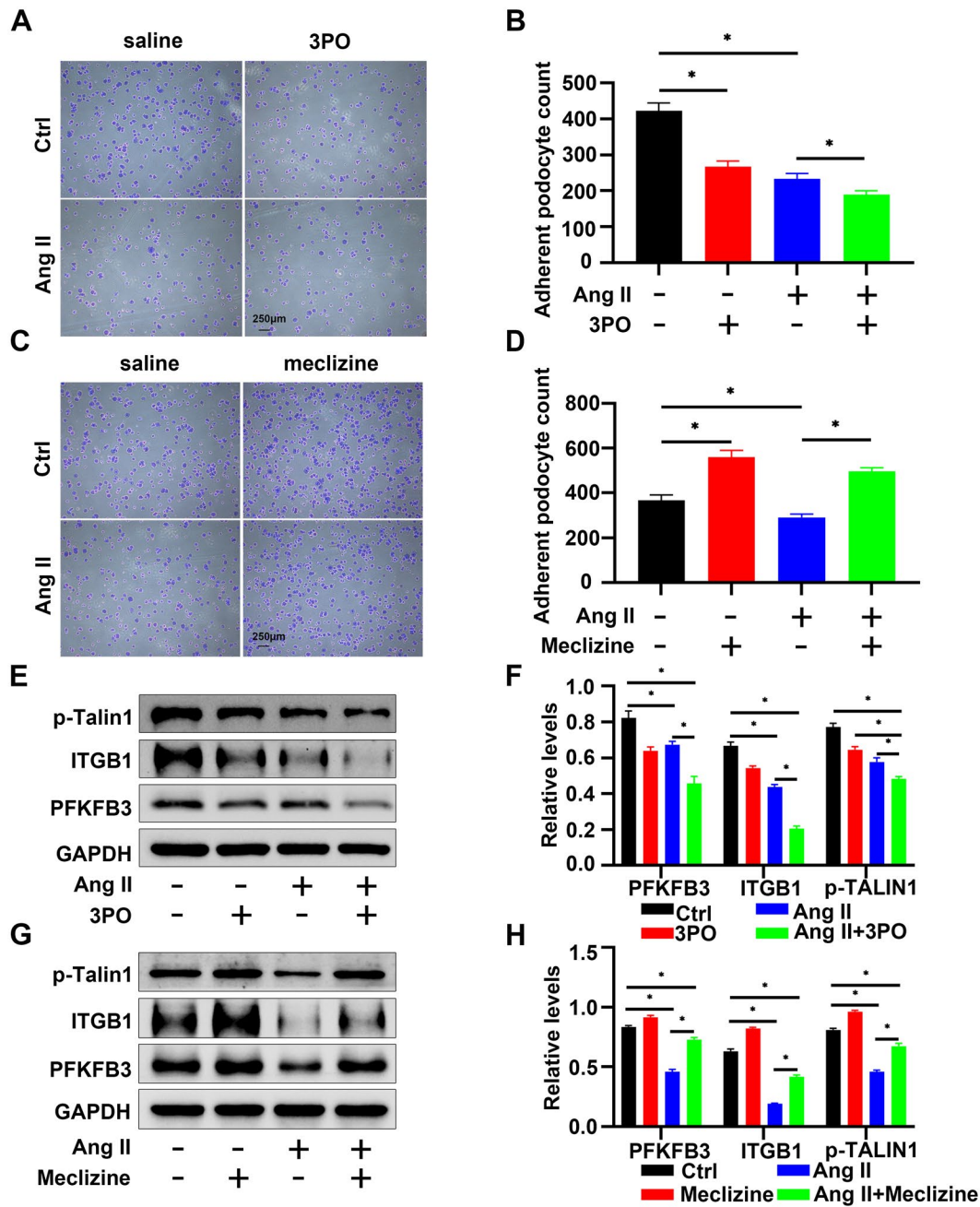
Figure 4. Regulation of podocyte adhesion was mediated by PFKFB3 *in vitro*. (A) Representative images of adhesion assays in different treatment groups of podocytes, Scale bars = 250 μm. (B) Quantitative determination of podocyte numbers in each group ($n = 5$), *$p < 0.05$. (C) Representative images of adhesion assays in different treatment groups of podocytes, Scale bars = 250 μm. (D) Quantitative determination of podocyte numbers in each group ($n = 5$), *$p < 0.05$. (E) Representative Western blots of phosphorylation of Talin1 and active ITGB1, and PFKFB3 in different treatment groups of podocytes. (F) Quantitative determination of Western blot of PFKFB3, ITGB1, p-Talin1 expression in each group ($n = 3$), *$p < 0.05$. (G) Representative Western blots of phosphorylation of Talin1 and active ITGB1, and PFKFB3 in different treatment groups of podocytes. (H) Quantitative determination of podocyte numbers in each group ($n = 3$), *$p < 0.05$.

transfected with PFKFB3 siRNA (Figure 5(C,D)), talin1 phosphorylation, and ITGB1 activity (Figure 5(E,F) and Figures S4 and S5). Our results also showed that Ang II promoted podocyte apoptosis and that PFKFB3 knockdown exacerbated Ang II-induced apoptosis (Figure S6). In summary, these findings highlight the potential inhibitory effects of PFKFB3 knockdown on talin1 phosphorylation, ITGB1 activity, and podocytes adhesion.

3.6. Overexpressed PFKFB3 ameliorated Ang II-induced podocyte detachment in vitro

We investigated the effects of PFKFB3 overexpression on podocyte adhesion *in vitro*. Transfecting podocytes with plasmids overexpressing PFKFB3 augmented podocyte adhesion, effectively mitigating the Ang II-induced reduction in the population of adherent podocytes (Figure 6(A,B)). Western blots to evaluate PFKFB3 expression in podocytes transfected
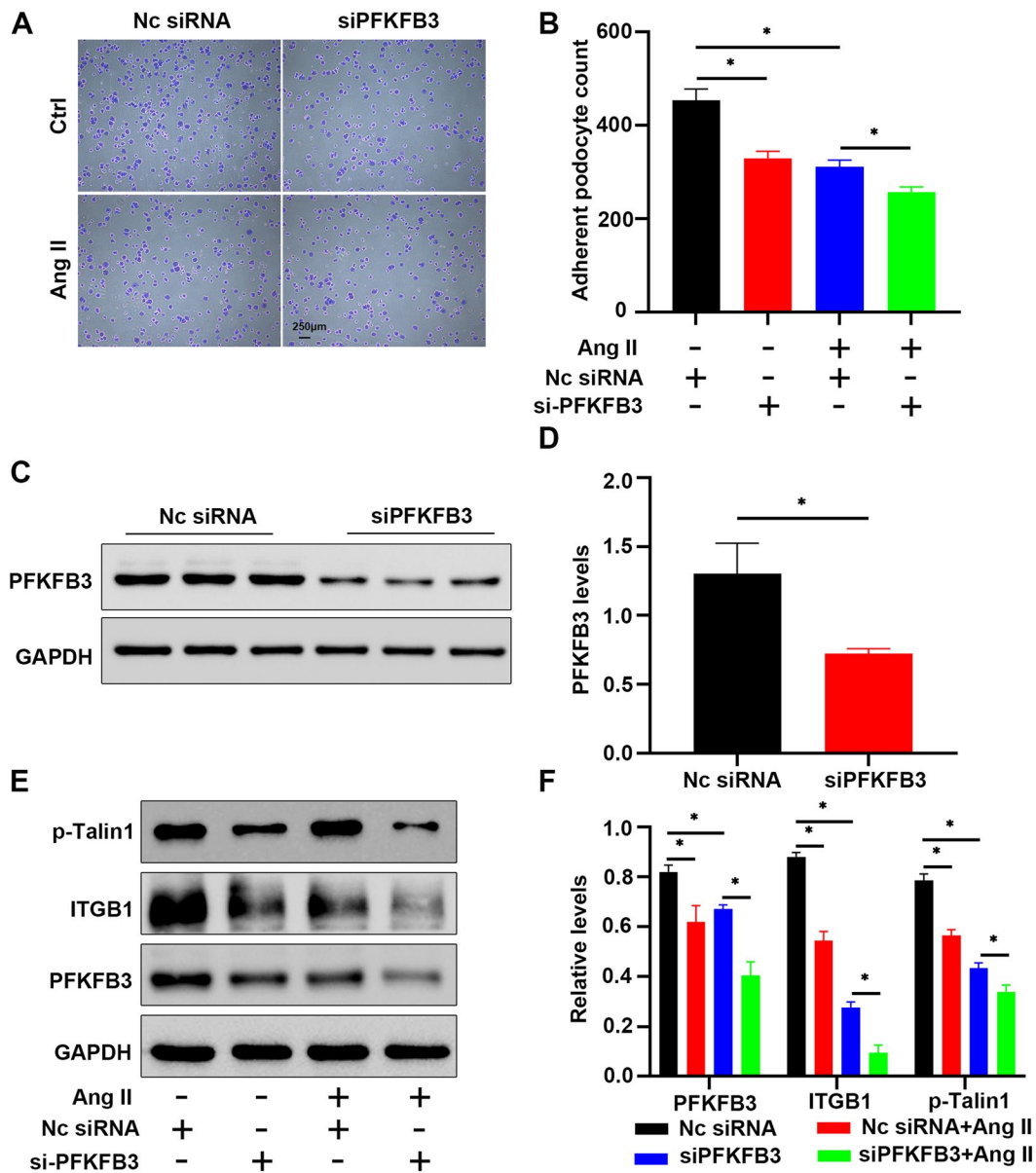
Figure 5. Angiotensin II-induced podocyte detachment *in vitro* is exacerbated by PFKFB3 knockdown. (A) Representative images of adhesion assays in NC-siRNA or siPFKFB3 transfected podocytes, Scale bars = 250 μm. (B) Quantitative determination of podocyte numbers in NC-siRNA or siPFKFB3 transfected podocytes (*n* = 3), *p < 0.05. (C) Representative Western blots of PFKFB3 in Nc-siRNA and siPFKFB3 transfected podocytes. (D) Quantitative determination of Western blot of PFKFB3 expression in podocytes transfected Nc-siRNA and siPFKFB3mice (*n* = 3), *p < 0.05. (E) Representative Western blots of phosphorylation of Talin1 and active ITGB1, and PFKFB3 in podocytes transfected Nc-siRNA and siPFKFB3. (F) Quantitative determination of Western blot of phosphorylation of Talin1 and active ITGB1, and PFKFB3 expression in transfected Nc-siRNA and siPFKFB3 podocytes (*n* = 3), *p < 0.05.

with plasmids overexpressing PFKFB3 revealed a substantial increase in PFKFB3 levels (Figure 6(C,D)). Transfecting podocytes with plasmids overexpressing PFKFB3 notably facilitated talin1 phosphorylation and ITGB1 activity, further counteracting the inhibitory effects of Ang II (Figure 6(E,F)). All these results indicated that upregulated PFKFB3 expression may promotes podocyte adhesion through the p-talin1 and ITGB1 pathways.

4. Discussion

The present study unveiled the role of PFKFB3 in podocyte detachment in mouse models *in vivo* and in cell cultures *in vitro* under Ang II stimulation. The expression of PFKFB3 was decreased in Ang II-treated podocytes. Mechanistically, decreased PFKFB3 expression and inactivation might suppress the p-talin1/ITGB1 signaling pathway, which aggravated podocyte loss and kidney injury. Conversely, upregulated and activated PFKFB3 improved podocyte adhesion, suggesting protective effects against podocyte damage in CKD.

Chronic kidney disease is a global public health obstacle with an increasing incidence [34]. The progression of CKD is often accompanied by a gradual decline in renal function, RAS activation, and glomerular pathological changes [35,36]. Podocytes are key components of the glomerular filtration barrier, playing a decisive role in
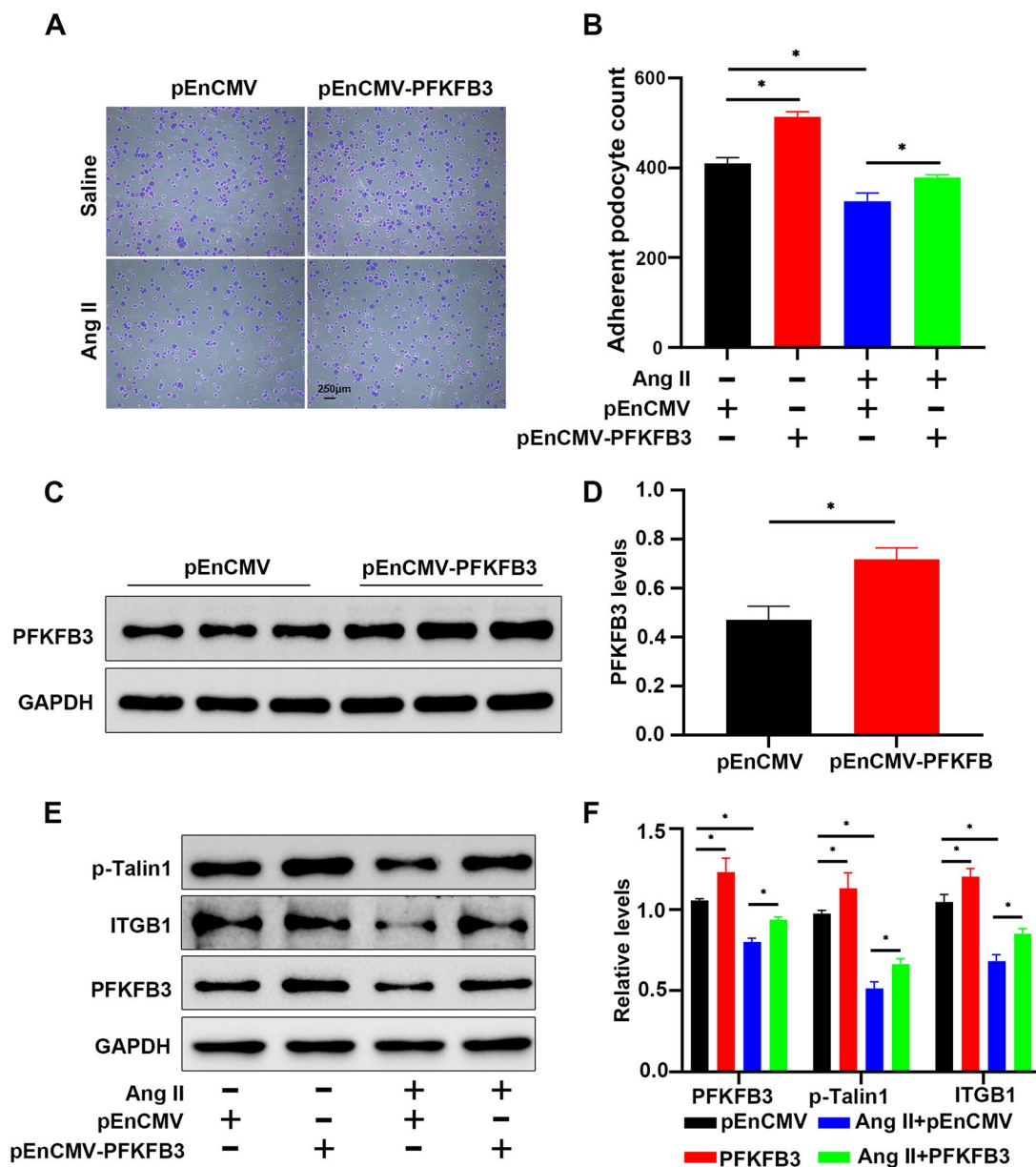
Figure 6. Overexpressed PFKFB3 ameliorated Ang II-induced podocyte detachment *in vitro*. (A) Representative images of adhesion assays in pEnCMV or pEnCMV-PFKFB3 transfected podocytes Scale bars = 300 μm. (B) Quantitative determination of podocyte numbers in pEnCMV or pEnCMV-PFKFB3 transfected podocytes ($n = 5$), *$p < 0.05$. (C) Representative Western blots of PFKFB3 in pEnCMV or pEnCMV-PFKFB3 transfected podocytes. (D) Quantitative determination of Western blot of PFKFB3 expression in pEnCMV or pEnCMV-PFKFB3 transfected podocytes. ($n = 3$), *$p < 0.05$. (E) Representative Western blots of phosphorylation of Talin1 and active ITGB1, and PFKFB3 in pEnCMV or pEnCMV-PFKFB3 transfected podocytes. (F) Quantitative determination of Western blots of phosphorylation of Talin1 and active ITGB1, and PFKFB3 expression in pEnCMV or pEnCMV-PFKFB3 transfected podocytes ($n = 3$), *$p < 0.05$.

maintaining normal kidney function. Podocyte damage and detachment from the basement membrane contribute to proteinuria and are considered critical for the initiation and progression of CKD [37,38]. Classical RAS contains various angiotensins, among which the principal effector is Ang II [39,40]. This hormone initiates CKD progression and induces podocyte damage, detachment and apoptosis through cellular metabolism and cytoskeleton remodeling [41–43]. Angiotensin II reduces the expression of podocyte adhesion molecules [44,45]. We confirmed here that Ang II causes podocyte detachment and loss, thus promoting proteinuria and glomerulosclerosis.

Cell adhesion molecules on the cell surface are involved in numerous physiological processes such as cell adhesion, survival, proliferation, epithelial–mesenchymal transition, and drug resistance [46]. Podocytes are anchored to the GBM *via* many types of cell adhesion molecules [47]. Podocyte detachment is a hallmark of kidney damage. Podocytes detach and become lost before apoptotic caspases are activated [8]. Reduced podocyte adhesion plays an important role in the progression of various podocyte diseases [48–50]. The molecular mechanisms underlying podocyte detachment remain under investigation. Non-catalytic region of tyrosine kinase adaptor protein 1 (Nck) functions in regulating podocyte

adhesion, controlling GBM composition, and sustaining filtration barrier integrity through actin organization [51]. The actin-binding protein, α-parvin, regulates the structure and composition of integrin adhesion complexes to prevent podocyte foot process effacement and detachment from the glomerular basement membrane [52]. Here we determined that PFKFB3, an important regulator of glycolysis, mediated podocyte adhesion *in vivo* and *in vitro*, thus revealing a new mechanism of podocyte detachment from the perspective of cellular metabolism.

The glycolytic enzyme PFKFB3 is involved in cancer, immunology, and inflammation [53–56], and its role in kidney disease has recently attracted attention. The cyclin-dependent kinase 4/retinoblastoma tumor suppressor pathway, activated by PFKFB3 mediates tubular cell death in cisplatin nephrotoxicity [57]. Mutations in PFKFB3 attenuates renal inflammation in diabetic kidney disease [58]. Interleukin-22 attenuates kidney damage by reprogramming the metabolism of renal tubular epithelial cells *via* PFKFB3 activation [18]. We found that PFKFB3 downregulation and pharmacological inhibition aggravated podocyte detachment and that its overexpression and activation played protective roles. This might represent a novel target for treating podocyte detachment in CKD *via* metabolic reprogramming.

Integrins are important cell adhesion molecules on the surface of podocytes and are closely associated with podocyte adhesion [59]. Integrins are heterodimers composed of non-covalently associated alpha and beta subunits that bind to extracellular matrix proteins and couple with intracellular signaling and cytoskeletal complexes [60]. The ITGB1 subunit is a vital member of the integrin family and is primarily responsible for podocyte adhesion [23,61,62]. The structural tail extension binding to GBM when ITGB1 is activated and folds to reduce such binding when ITGB1 is inactivated. This causes adherent podocytes recede [21]. We found here that decreased expression of ITGB1 and phosphorylated talin1 aggravated the detachment of podocytes incubated with Ang II. Mechanistically, decreased PFKFB3 expression could mediate dysregulated ITGB1 activation and suppressed talin1 phosphorylation. In contrast, upregulated and activated PFKFB3 may promote talin1 phosphorylation and further alleviated podocyte detachment. Altered cellular metabolic states impact the expression of adhesion molecules.

Angiotensin II promotes the expression of hypoxia-inducible factor-1α [63]. A feedback loop exists between PFKFB3 and HIF-1α, and a HIF-1α blockade restricts PFKFB3 enhancement [64]. However, details of the mechanism underlying PFKFB3 downregulation by Ang II requires further investigation. Our study has several limitations: In this study, only Ang II-infused mouse models and Ang II-stimulated podocytes were used to investigate the effects and mechanisms. Therefore, our findings require validation in podocyte PFKFB3 conditional knockout mice and other mouse models of renal injury in forthcoming experiments. Although previous literature reports have demonstrated that PFKFB3 is capable of activating CDK1 and have indicated a direct interaction between CDK1 and p-Talin1 [19,20], the specific mechanism of PFKFB3 regulating p-Talin1 expression still needs to be further studied.

In conclusion, our study shows that inhibition of PFKFB3 decreases Ang II-mediated podocyte adhesion, possibly by inhibiting the Talin1-ITGB1 signaling pathway, which induces renal injury. These findings provide new insights into the mechanisms of altered RAS-activated podocyte adhesion and offers the potential for new modalities to treat podocyte damage in CKD.

Author contributions

X.H., Z.C., and G.D. designed the study. X.H. and Z.L. assisted with the animal experiments. X.H., Z.Zhu., Y.H., J.F., X.Y., Z.Zhang., and J.H. performed the experiments. X.H., Z.Zhu., Q.L., J.F., J.H., and W.L. analyzed and interpreted the data. X.H., Z.C., and G.D. drafted the manuscript. All authors have contributed to the manuscript and approved the submitted version.

Disclosure statement

No potential conflict of interest was reported by the author(s).

Funding

Data availability statement

All the data supporting this research are available from the corresponding author upon reasonable request.

References

[1] Lennon R, Randles MJ, Humphries MJ. The importance of podocyte adhesion for a healthy glomerulus. Front Endocrinol. 2014;5:1. doi: 10.3389/fendo.2014.00160.

[2] Trimarchi H. Mechanisms of podocyte detachment, podocyturia, and risk of progression of glomerulopathies. Kidney Dis. 2020;6(5):324–13. doi: 10.1159/000507997.

[3] Ren Q, Yu S, Zeng H, et al. The role of PTEN in puromycin aminonucleoside-induced podocyte injury. Int J Med Sci. 2022;19(9):1451–1459. doi: 10.7150/ijms.72988.

[4] Fukuda A, Wickman LT, Venkatareddy MP, et al. Angiotensin II-dependent persistent podocyte loss from destabilized glomeruli causes progression of end stage kidney disease. Kidney Int. 2012;81(1):40–55. doi: 10.1038/ki.2011.306.

[5] Gil CL, Hooker E, Larrivee B. Diabetic kidney disease, endothelial damage, and podocyte-endothelial crosstalk. Kidney Med. 2021;3(1):105–115. doi: 10.1016/j.xkme.2020.10.005.

[6] Kopp JB, Anders HJ, Susztak K, et al. Podocytopathies. Nat Rev Dis Primers. 2020;6(1):68. doi: 10.1038/s41572-020-0196-7.

[7] Yin L, Yu L, He JC, et al. Controversies in podocyte loss: death or detachment? Front Cell Dev Biol. 2021;9:771931. doi: 10.3389/fcell.2021.771931.

[8] Yamamoto K, Okabe M, Tanaka K, et al. Podocytes are lost from glomeruli before completing apoptosis. Am J Physiol Renal Physiol. 2022;323(5):F515–f526. doi: 10.1152/ajprenal.00080.2022.

[9] Kang JS, Lee SJ, Lee JH, et al. Angiotensin II-mediated MYH9 downregulation causes structural and functional podocyte injury in diabetic kidney disease. Sci Rep. 2019;9(1):7679. doi: 10.1038/s41598-019-44194-3.

[10] Marquez A, Wysocki J, Pandit J, et al. An update on ACE2 amplification and its therapeutic potential. Acta Physiol. 2021;231(1):e13513. doi: 10.1111/apha.13513.

[11] Urushihara M, Kagami S. Role of the intrarenal renin-angiotensin system in the progression of renal disease. Pediatr Nephrol. 2017;32(9):1471–1479. doi: 10.1007/s00467-016-3449-7.

[12] Pilvankar MR, Higgins MA, Ford Versypt AN. Mathematical model for glucose dependence of the local renin-angiotensin system in podocytes. Bull Math Biol. 2018;80(4):880–905. doi: 10.1007/s11538-018-0408-4.

[13] Malek V, Suryavanshi SV, Sharma N, et al. Potential of renin-angiotensin-aldosterone system modulations in diabetic kidney disease: old players to new hope!. Rev Physiol Biochem Pharmacol. 2021;179:31–71.

[14] Yang Y, Yang Q, Yang J, et al. Angiotensin II induces cholesterol accumulation and injury in podocytes. Sci Rep. 2017;7(1):10672. doi: 10.1038/s41598-017-09733-w.

[15] Marquez E, Riera M, Pascual J, et al. Renin-angiotensin system within the diabetic podocyte. Am J Physiol Renal Physiol. 2015;308(1):F1–F10. doi: 10.1152/ajprenal.00531.2013.

[16] Shi L, Pan H, Liu Z, et al. Roles of PFKFB3 in cancer. Signal Transduct Target Ther. 2017;2:17044.

[17] Sakakibara R, Kato M, Okamura N, et al. Characterization of a human placental fructose-6-phosphate, 2-kinase/fructose-2,6-bisphosphatase. J Biochem. 1997;122(1):122–128. doi: 10.1093/oxfordjournals.jbchem.a021719.

[18] Chen W, Shen Y, Fan J, et al. IL-22-mediated renal metabolic reprogramming via PFKFB3 to treat kidney injury. Clin Transl Med. 2021;11(2):e324.

[19] Yalcin A, Clem BF, Imbert-Fernandez Y, et al. 6-Phosphofructo-2-kinase (PFKFB3) promotes cell cycle progression and suppresses apoptosis via Cdk1-mediated phosphorylation of p27. Cell Death Dis. 2014;5(7):e1337. doi: 10.1038/cddis.2014.292.

[20] Gough RE, Jones MC, Zacharchenko T, et al. Talin mechanosensitivity is modulated by a direct interaction with cyclin-dependent kinase-1. J Biol Chem. 2021;297(1):100837. doi: 10.1016/j.jbc.2021.100837.

[21] Jin JK, Tien PC, Cheng CJ, et al. Talin1 phosphorylation activates beta1 integrins: a novel mechanism to promote prostate cancer bone metastasis. Oncogene. 2015;34(14):1811–1821. doi: 10.1038/onc.2014.116.

[22] Chen CA, Chang JM, Yang YL, et al. Macrophage migration inhibitory factor regulates integrin-beta1 and cyclin D1 expression via ERK pathway in podocytes. Biomed Pharmacother. 2020;124:109892. doi: 10.1016/j.biopha.2020.109892.

[23] Lay AC, Hale LJ, Stowell-Connolly H, et al. IGFBP-1 expression is reduced in human type 2 diabetic glomeruli and modulates β1-integrin/FAK signalling in human podocytes. Diabetologia. 2021;64(7):1690–1702. doi: 10.1007/s00125-021-05427-1.

[24] Pozzi A, Jarad G, Moeckel GW, et al. Beta1 integrin expression by podocytes is required to maintain glomerular structural integrity. Dev Biol. 2008;316(2):288–301. doi: 10.1016/j.ydbio.2008.01.022.

[25] Spiess M, Hernandez-Varas P, Oddone A, et al. Active and inactive β1 integrins segregate into distinct nanoclusters in focal adhesions. J Cell Biol. 2018;217(6):1929–1940. doi: 10.1083/jcb.201707075.

[26] Wang L, Cao Y, Gorshkov B, et al. Ablation of endothelial Pfkfb3 protects mice from acute lung injury in LPS-induced endotoxemia. Pharmacol Res. 2019;146:104292. doi: 10.1016/j.phrs.2019.104292.

[27] Pekkonen P, Alve S, Balistreri G, et al. Lymphatic endothelium stimulates melanoma metastasis and invasion via MMP14-dependent Notch3 and beta1-integrin activation. Elife. 2018;7:32490. doi: 10.7554/eLife.32490.

[28] Cruys B, Wong BW, Kuchnio A, et al. Glycolytic regulation of cell rearrangement in angiogenesis. Nat Commun. 2016;7:12240. doi: 10.1038/ncomms12240.

[29] Yang Q, Xu J, Ma Q, et al. Disruption of endothelial Pfkfb3 ameliorates diet-induced murine insulin resistance. J Endocrinol. 2021;250(3):93–104. doi: 10.1530/JOE-20-0524.

[30] Cao Y, Zhang X, Wang L, et al. PFKFB3-mediated endothelial glycolysis promotes pulmonary hypertension. Proc Natl Acad Sci U S A. 2019;116(27):13394–13403. doi: 10.1073/pnas.1821401116.

[31] Gao L, Wang C, Qin B, et al. 6-phosphofructo-2-kinase/fructose-2,6-bisphosphatase suppresses neuronal apoptosis by increasing glycolysis and cyclin-dependent kinase 1-Mediated phosphorylation of p27 after traumatic spinal cord injury in rats. Cell Transplant. 2020;29:963689720950226. doi: 10.1177/0963689720950226.

[32] Rauch C, Feifel E, Kern G, et al. Differentiation of human iPSCs into functional podocytes. PLoS One. 2018;13(9):e0203869. doi: 10.1371/journal.pone.0203869.

[33] Mundel P, Heid HW, Mundel TM, et al. Synaptopodin: an actin-associated protein in telencephalic dendrites and renal podocytes. J Cell Biol. 1997;139(1):193–204. doi: 10.1083/jcb.139.1.193.

[34] Bikbov B, Purcell CA, Levey AS, et al. Global, regional, and national burden of chronic kidney disease, 1990–2017: a systematic analysis for the global burden of disease study 2017. Lancet. 2020;395(10225):709–733. doi: 10.1016/S0140-6736(20)30045-3.

[35] Yang Q, Hu J, Yang Y, et al. Sirt6 deficiency aggravates angiotensin II-induced cholesterol accumulation and injury in podocytes. Theranostics. 2020;10(16):7465–7479. doi: 10.7150/thno.45003.

[36] Feng J, Chen Z, Ma Y, et al. AKAP1 contributes to impaired mtDNA replication and mitochondrial dysfunction in podocytes of diabetic kidney disease. Int J Biol Sci. 2022;18(10):4026–4042. doi: 10.7150/ijbs.73493.

[37] Gao S, Cui Z, Zhao MH. Complement C3a and C3a receptor activation mediates podocyte injuries in the mechanism of primary membranous nephropathy. J Am Soc Nephrol. 2022;33(9):1742–1756. doi: 10.1681/ASN.2021101384.

[38] Schunk SJ, Floege J, Fliser D, et al. WNT-β-catenin signalling - a versatile player in kidney injury and repair.

Nat Rev Nephrol. 2021;17(3):172–184. doi: 10.1038/s41581-020-00343-w.

[39] Carey RM, Siragy HM. Newly recognized components of the renin-angiotensin system: potential roles in cardiovascular and renal regulation. Endocr Rev. 2003;24(3):261–271. doi: 10.1210/er.2003-0001.

[40] Chow BSM, Allen TJ. Angiotensin II type 2 receptor (AT2R) in renal and cardiovascular disease. Clin Sci (Lond). 2016;130(15):1307–1326. doi: 10.1042/CS20160243.

[41] Chen Z, Liang W, Hu J, et al. Sirt6 deficiency contributes to mitochondrial fission and oxidative damage in podocytes via ROCK1-Drp1 signalling pathway. Cell Prolif. 2022;55(10):e13296.

[42] Luo Z, Chen Z, Zhu Z, et al. Angiotensin II induces podocyte metabolic reprogramming from glycolysis to glycerol-3-phosphate biosynthesis. Cell Signal. 2022;99:110443. doi: 10.1016/j.cellsig.2022.110443.

[43] Erichsen L, Thimm C, Bohndorf M, et al. Activation of the renin-angiotensin system disrupts the cytoskeletal architecture of human urine-derived podocytes. Cells. 2022;11(7):1095. doi: 10.3390/cells11071095.

[44] Tian L, Coletti D, Li ZL. Angiotensin II induces the exocytosis of galectin-3 via integrin αv/AKT/NF-κB signaling pathway. Eur Rev Med Pharmacol Sci. 2019;23(13):5949–5957.

[45] Lang P-P, Bai J, Zhang Y-L, et al. Blockade of intercellular adhesion molecule-1 prevents angiotensin II-induced hypertension and vascular dysfunction. Lab Invest. 2020;100(3):378–386. doi: 10.1038/s41374-019-0320-z.

[46] Ruan Y, Chen L, Xie D, et al. Mechanisms of cell adhesion molecules in endocrine-related cancers: a concise outlook. Front Endocrinol. 2022;13:865436. doi: 10.3389/fendo.2022.865436.

[47] Sachs N, Sonnenberg A. Cell-matrix adhesion of podocytes in physiology and disease. Nat Rev Nephrol. 2013;9(4):200–210. doi: 10.1038/nrneph.2012.291.

[48] Artelt N, Ludwig TA, Rogge H, et al. The role of palladin in podocytes. J Am Soc Nephrol. 2018;29(6):1662–1678. doi: 10.1681/ASN.2017091039.

[49] Farmer LK, Rollason R, Whitcomb DJ, et al. TRPC6 binds to and activates calpain, independent of its channel activity, and regulates podocyte cytoskeleton, cell adhesion, and motility. J Am Soc Nephrol. 2019;30(10):1910–1924. doi: 10.1681/ASN.2018070729.

[50] Zhang L, Wen Z, Han L, et al. Research progress on the pathological mechanisms of podocytes in diabetic nephropathy. J Diabetes Res. 2020;2020:7504798.

[51] Martin CE, Phippen NJ, Keyvani Chahi A, et al. Complementary Nck1/2 signaling in podocytes controls actinin-4-Mediated actin organization, adhesion, and basement membrane composition. J Am Soc Nephrol. 2022;33(8):1546–1567. doi: 10.1681/ASN.2021101343.

[52] Rogg M, Maier JI, Van Wymersch C, et al. α-Parvin defines a specific integrin adhesome to maintain the glomerular filtration barrier. J Am Soc Nephrol. 2022;33(4):786–808. doi: 10.1681/ASN.2021101319.

[53] Wang B, Li D, Ilnytskyy Y, et al. A miR-34a-guided, tRNA-derived, piR_019752-like fragment (tRiMetF31) suppresses migration and angiogenesis of breast cancer cells via targeting PFKFB3. Cell Death Discov. 2022;8(1):355. doi: 10.1038/s41420-022-01054-w.

[54] Hu M, Bao R, Lin M, et al. ALK fusion promotes metabolic reprogramming of cancer cells by transcriptionally upregulating PFKFB3. Oncogene. 2022;41(40):4547–4559. doi: 10.1038/s41388-022-02453-0.

[55] Wang S, Yu H, Gao J, et al. PALMD regulates aortic valve calcification via altered glycolysis and NF-κB-mediated inflammation. J Biol Chem. 2022;298(5):101887. doi: 10.1016/j.jbc.2022.101887.

[56] Icard P, Alifano M, Donnadieu E, et al. Fructose-1,6-bisphosphate promotes PI3K and glycolysis in T cells? Trends Endocrinol Metab. 2021;32(8):540–543. doi: 10.1016/j.tem.2021.04.013.

[57] Wen L, Wei Q, Livingston MJ, et al. PFKFB3 mediates tubular cell death in cisplatin nephrotoxicity by activating CDK4. Transl Res. 2023;253:31–40. doi: 10.1016/j.trsl.2022.10.001.

[58] Song C, Wang S, Fu Z, et al. IGFBP5 promotes diabetic kidney disease progression by enhancing PFKFB3-mediated endothelial glycolysis. Cell Death Dis. 2022;13(4):340. doi: 10.1038/s41419-022-04803-y.

[59] Shen A-R, Zhong X, Tang T-T, et al. Integrin, exosome and kidney disease. Front Physiol. 2020;11:627800. doi: 10.3389/fphys.2020.627800.

[60] Kadry YA, Calderwood DA. Chapter 22: structural and signaling functions of integrins. Biochim Biophys Acta Biomembr. 2020;1862(5):183206. doi: 10.1016/j.bbamem.2020.183206.

[61] Chen C-A, Chang J-M, Chang E-E, et al. TGF-β1 modulates podocyte migration by regulating the expression of integrin-β1 and -β3 through different signaling pathways. Biomed Pharmacother. 2018;105:974–980. doi: 10.1016/j.biopha.2018.06.054.

[62] Yuan X, Wang W, Wang J, et al. Down-regulation of integrin β1 and focal adhesion kinase in renal glomeruli under various hemodynamic conditions. PLoS One. 2014;9(4):e94212. doi: 10.1371/journal.pone.0094212.

[63] Huang H, Fan Y, Gao Z, et al. HIF-1α contributes to ang II-induced inflammatory cytokine production in podocytes. BMC Pharmacol Toxicol. 2019;20(1):59. doi: 10.1186/s40360-019-0340-8.

[64] Long Q, Zou X, Song Y, et al. PFKFB3/HIF-1α feedback loop modulates sorafenib resistance in hepatocellular carcinoma cells. Biochem Biophys Res Commun. 2019;513(3):642–650. doi: 10.1016/j.bbrc.2019.03.109.